J Struct Funct Genomics (2014) 15:173–180
DOI 10.1007/s10969-014-9183-0

Crystal structure of tRNA m^{1}A58 methyltransferase TrmI from *Aquifex aeolicus* in complex with *S*-adenosyl-L-methionine

Mitsuo Kuratani · Tatsuo Yanagisawa · Ryohei Ishii · Michiyo Matsuno · Shu-Yi Si · Kazushige Katsura · Ryoko Ushikoshi-Nakayama · Rie Shibata · Mikako Shirouzu · Yoshitaka Bessho · Shigeyuki Yokoyama

Received: 4 March 2014 / Accepted: 28 May 2014 / Published online: 4 June 2014

Abstract The N^1-methyladenosine residue at position 58 of tRNA is found in the three domains of life, and contributes to the stability of the three-dimensional L-shaped tRNA structure. In thermophilic bacteria, this modification is important for thermal adaptation, and is catalyzed by the tRNA m^{1}A58 methyltransferase TrmI, using *S*-adenosyl-L-methionine (AdoMet) as the methyl donor. We present the 2.2 Å crystal structure of TrmI from the extremely thermophilic bacterium *Aquifex aeolicus*, in complex with AdoMet. There are four molecules per asymmetric unit, and they form a tetramer. Based on a comparison of the AdoMet binding mode of *A. aeolicus* TrmI to those of the *Thermus thermophilus* and *Pyrococcus abyssi* TrmIs, we discuss their similarities and differences. Although the binding modes to the N6 amino group of the adenine moiety of AdoMet are similar, using the side chains of acidic residues as well as hydrogen bonds, the positions of the amino acid residues involved in binding are diverse among the TrmIs from *A. aeolicus*, *T. thermophilus*, and *P. abyssi*.

Keywords AdoMet · tRNA modification enzyme · Methylation · X-ray crystal structure · Structural genomics

Abbreviations

AdoMet	*S*-Adenosyl-L-methionine
AdoHcy	*S*-Adenosyl-L-homocysteine
m^{1}A	N^1-Methyladenosine
m^{1}G	N^1-Methylguanosine
m^{1}I	N^1-Methylinosine
m^{3}C	N^3-Methylcytidine
m$^3\Psi$	N^3-Methylpseudouridine
m^{3}U	N^3-Methyluridine
IPTG	Isopropyl-1-thio-β-D-galactopyranoside
tRNA	Transfer RNA
PDB	Protein Data Bank
RMSD	Root-mean-square-deviation

Introduction

Posttranscriptional modifications alter the characteristics of tRNAs in various manners, to fine-tune their functions. The modified nucleoside N^1-methyladenosine is found at four positions: position 9 of mammalian mitochondrial tRNAs, position 14 of mammalian cytoplasmic tRNA^{Phe}, position 22 of tRNA in some bacteria, and position 58 of tRNA in

M. Kuratani · T. Yanagisawa · R. Ishii · M. Matsuno · S.-Y. Si · K. Katsura · R. Ushikoshi-Nakayama · R. Shibata · M. Shirouzu · Y. Bessho · S. Yokoyama (✉)
RIKEN Genomic Sciences Center, 1-7-22 Suehiro-cho, Tsurumi-ku, Yokohama 230-0045, Japan
e-mail: yokoyama@riken.jp

M. Kuratani · T. Yanagisawa · S. Yokoyama
RIKEN Structural Biology Laboratory, 1-7-22 Suehiro-cho, Tsurumi-ku, Yokohama 230-0045, Japan

R. Ishii
Department of Biophysics and Biochemistry, Graduate School of Science, The University of Tokyo, 2-11-16 Yayoi, Bunkyo-ku, Tokyo 113-0032, Japan

K. Katsura · M. Shirouzu
Division of Structural and Synthetic Biology, RIKEN Center for Life Science Technologies, 1-7-22 Suehiro-cho, Tsurumi-ku, Yokohama 230-0045, Japan

Y. Bessho
RIKEN SPring-8 Center, 1-1-1 Kouto, Sayo, Hyogo 679-5148, Japan

the three domains of life [1]. The N^1-methylation of adenosine abrogates its ability to form a standard Watson–Crick base pair, as also found with m^1G, m^1I, m^3C, m^3U, and $m^3\Psi$. Indeed, reverse transcriptases read m^1A with very low efficiency, and those in the HIV-1 and Molony murine leukemia viruses utilize the host's tRNA bearing m^1A for their replication [2–5].

In the absence of the m^1A9 modification, mammalian mitochondrial $tRNA^{Lys}$ could adopt an extended hairpin structure that is unproductive in translation, since an undesired base pair between A9 and U64 is tolerated [6, 7]. In yeast, the strain with a defective m^1A58 modification is nonviable, because the initiator $tRNA^{Met}$ is degraded [8]. In the native yeast tRNA, the m^1A58 of the initiator $tRNA^{Met}$ forms the reverse Hoogsteen base pair with A54, which increases the stability of the three-dimensional structure, while the m^1A58 in the other 19 tRNAs forms the reverse Hoogsteen base pair with T54 [9–11]. In the thermophilic bacterium *Thermus thermophilus*, inactivation of the *trmI* gene results in a thermosensitive phenotype, suggesting that the m^1A58 modification is important for both thermal adaptation and tRNA stability [12]. The m^1A58 residue was analyzed by NMR and IR spectral studies, which considered the ^1H, ^{13}C, and ^{15}N chemical shifts, the consistency of the sugar pucker and glycosidic conformations with those of the X-ray structure, and the character of the bond between the C6 and N6 atoms [13, 14]. Based on the results, the m^1A58 residue in the native tRNA was deduced to be fully protonated, with its charge probably dislocalized from the quaternary N1 atom toward the C6, C5, and C4 atoms. The protonated state of the m^1A58 residue is characteristic of the Mg^{2+}-bound native state, and the partial charge in the tRNA elbow region may affect its interaction with the translational machinery [13, 14]. Therefore, the m^1A58 modification of tRNA is important for stabilizing the L-shaped structure and for efficient translation [15].

The methyl group of m^1A58 is transferred from the methyl donor *S*-adenosyl-L-methionine (AdoMet) by the TrmI homotetramer in bacteria and archaea, and by the Trm6/Trm61 α2/β2 heterotetramer complex in eukaryotes [8, 12]. The coordinated structural genomics projects on proteins from *Mycobacterium tuberculosis* determined the first structure of TrmI, as the conserved hypothetical methyltransferase Rv2118c [16]. At the same time, an in silico fold prediction study was reported [17]. Subsequently, the crystal structure of the catalytic domain (residues 70–250) of the TrmI tetramer from *Pyrococcus abyssi* revealed its mechanism of thermal stabilization, using intersubunit disulfide bonds [18]. The crystal structure of TrmI from *T. thermophilus* [19] was determined and complemented by biophysical characterizations, which revealed the tRNA binding stoichiometry per TrmI tetramer [19]. The crystal structure of full-length TrmI from *P. abyssi* was reported with further biochemical characterization of the region specificities [20]. Presently, eight PDB datasets from six species are available, and their structural architectures have been compared [21]. Comprehensive structural genomics projects on a specific organism, typified by that on *M. tuberculosis* [22], have provided the structural basis to characterize the biological functions of the proteome, including conserved proteins with unknown functions. On the other hand, comparative analyses of large numbers of orthologous and homologous structures, including some acquired by high-throughput capability and successful structural genomics [23–25], will lead to further understanding of the structure–function relationships of proteins and facilitate applications, including protein engineering and drug design. Here, we report the crystal structure of TrmI from *Aquifex aeolicus* in the complex with AdoMet, determined at 2.2 Å resolution. The overall tetrameric architecture is quite similar to the structures of TrmIs from other species [21]. We examined the similarities and differences in the AdoMet recognition by *A. aeolicus* TrmI, as compared to those by the TrmIs from *T. thermophilus* and *P. abyssi*.

Materials and methods

Cloning, expression, and purification of *A. aeolicus* TrmI

The aq_311 gene, encoding the *A. aeolicus* TrmI protein (gi: 15605836) comprising 248 residues, was amplified by PCR using *A. aeolicus* VF5 genomic DNA and cloned into the pET-21a expression vector (Merck Novagen, Darmstadt, Germany). The expression vector was transformed into the *E. coli* Rosetta™ (DE3) strain (Merck Novagen). The cells were cultured at 37 °C in LB medium, supplemented with 30 μg/ml chloramphenicol and 50 μg/ml ampicillin. The protein expression was induced by 0.5 mM IPTG. Following an overnight incubation, the cells were harvested by centrifugation and stored at −80 °C. The cells were resuspended in 20 mM Tris–HCl buffer (pH 8.0), containing 300 mM NaCl, 5 mM $MgCl_2$, 0.5 mM EDTA, and 1 mM DTT, and were lysed by sonication on ice. The cell lysate was heat-treated at 70 °C for 30 min to denature most of the *E. coli* proteins, and was centrifuged at 15,000×*g* for 20 min at 4 °C. The supernatant was desalted by dialysis against 20 mM Tris–HCl buffer (pH 8.0) containing 1 mM DTT, and applied to a HiTrap Q column (GE Healthcare Biosciences), equilibrated with the same buffer. The protein was eluted with a linear gradient (0–1.0 M) of NaCl, and the target fractions, which eluted around 0.4 M NaCl, were collected. Ammonium sulfate

was added to the sample, which was applied to a Resource PHE column (GE Healthcare Biosciences), equilibrated with 20 mM Tris–HCl buffer (pH 8.0) containing 1.2 M ammonium sulfate and 1 mM DTT, and was eluted with a decreasing linear (1.2–0 M) gradient of ammonium sulfate. The target fractions, which were eluted in 0.6–0.3 M ammonium sulfate, were collected and desalted by dialysis. The sample was applied to a Mono S column (GE Healthcare Biosciences), equilibrated with 20 mM Tris–HCl buffer (pH 8.0) containing 1 mM DTT, and was eluted by a linear (0–1.0 M) gradient of NaCl. The fraction that eluted at 0.3 M was concentrated and applied to a HiLoad 16/60 Superdex 75 pg column (GE Healthcare Biosciences), equilibrated with 20 mM Tris–HCl buffer (pH 8.0) containing 150 mM NaCl and 1 mM DTT. The gel filtration elution profile showed one peak at 50 ml, which corresponds to 0.41 column volumes. The protein sample was concentrated to 15 mg/ml by ultrafiltration. The protein purification was analyzed by SDS-PAGE. The electrophoretic mobility of *A. aeolicus* TrmI is almost the same as that of a marker (29 kDa), in agreement with its theoretical molecular weight (28.7 kDa). The final yield was 2.2 mg/l of culture.

Crystallization and data collection

The *A. aeolicus* TrmI protein at 10–12 mg/ml concentrations, in 20 mM Tris–HCl buffer (pH 8.0) containing 150 mM NaCl, 1 mM DTT, and 2 mM AdoMet, was used for crystallization. Initial crystallization screening was performed in 1:1 sitting-drop vapor-diffusion reactions at 20 °C, by mixing 1 µl protein solution with 1 µl reservoir solution. The crystals were grown in 0.1 M Tris–HCl buffer (pH 8.4) and 20 % ethanol. The crystals were transferred to 0.1 M Tris–HCl buffer (pH 8.4), 20 % ethanol, and 35 % ethylene glycol for cryoprotection, prior to flash-cooling in liquid nitrogen for data collection. The native dataset was collected on beamline BL41XU at SPring-8 (Table 1). Data collected from a single crystal at 100 K were processed with the *HKL2000* program [26].

Structure solution and refinement

The phase was determined by the molecular replacement method, using the coordinates of TrmI from *Thermotoga maritima* (PDB ID: 1O54) as the starting model, with the program MOLREP [27]. The model was completed using iterative cycles of manual rebuilding in Coot [28] and computational refinement at 2.2 Å in *Refmac5* [29] (Table 1).

Table 1 X-ray data and refinement statistics

	A. aeolicus TrmI
Crystal parameters	
Space group	$P\ 2_1\ 2_1\ 2_1$
Cell dimensions	
a, b, c (Å)	69.8, 97.2, 212.7
α, β, γ (°)	90, 90, 90
Matthews coefficient ($Å^3$/Da)	3.14
Solvent content (%)	60.9
Data collection	
Wavelength (Å)	1.00
Resolution (Å)	50–2.2 (2.28–2.2)
R_{sym} (%)[a]	3.3 (43.9)
No. of unique reflections	68,373
No. of reflections in R_{free} set	3,597
Mean redundancy	6.6 (3.6)
Overall completeness (%)	96.7 (77.0)
Mean I/σ	23.7 (4.1)
Refinement residuals	
Resolution (Å)	50–2.2 (2.26–2.2)
R_{free} (%)[b]	23.0 (26.3)
R_{work} (%)[b]	19.4 (20.7)
Completeness (%)	96.8 (75.3)
Model quality	
RMSD bond lengths (Å)	0.008
RMSD bond angles (°)	1.1
Molprobity Ramachandran distribution	
Most favored (%)	98.6
Allowed (%)	1.4
Disallowed (%)	0.0
Mean main chain B-factor ($Å^2$)	26.5
Mean overall B-factor ($Å^2$)	31.7
Mean ligand B-factor ($Å^2$)	32.3
Mean solvent B-factor ($Å^2$)	31.2
Model contents	
Protomers in ASU	4
Protein residues	2–248
Ligands	4 AdoMet
No. of protein atoms	8,092
No. of ligand atoms	108
No. of water molecules	537
PDB accession code	2YVL

RMSD root-mean-square-deviation, *ASU* asymmetric unit

[a] $R_{sym} = \Sigma_{hkl}\ \Sigma_j|I_j(hkl) - \langle I_j(hkl)\rangle|/\Sigma_{hkl}\Sigma_j I(hkl)$, where $I_j(hkl)$ and $\langle I_j(hkl)\rangle$ are the intensity of measurement j and the mean intensity for the reflection with indices hkl, respectively

[b] $R_{work,\ free} = \Sigma|F_{obs} - kF_{calc}|/\Sigma_{hkl}F_{obs}$, where k is a scale factor, and the crystallographic R-factor is calculated including (R_{work}) and excluding (R_{free}) reflections. In each refinement, free reflections consist of 5 % of the total reflections

Structure validation and deposition

The structure validation of the model is summarized in Table 1. The atomic coordinates and structure factors have been deposited in the Protein Data Bank, under the accession code 2YVL.

Sedimentation velocity ultracentrifugation analysis

The *A. aeolicus* TrmI protein, at a 1 mg/ml concentration in 20 mM Tris–HCl buffer (pH 8.0) containing 150 mM NaCl and 1 mM DTT, was analyzed by ultracentrifugation at 20 °C, in a ProteomeLab XL-I ultracentrifuge (Beckman Coulter) with the An-60 Ti analytical rotor. The sample was ultracentrifuged at 40,000 rpm, and the absorbance at 280 nm was measured. The data were analyzed and the distribution c(M) was calculated by Sedfit [30].

Results and discussion

The crystal structure of *A. aeolicus* TrmI was determined at 2.2 Å resolution by the molecular replacement method, and was refined to R_{work} and R_{free} factors of 19.6 and 23.0 %, respectively (Table 1). The asymmetric unit contains four protomers (A–D) (Fig. 1a) and four AdoMet molecules. The electron density was interpretable for 247 residues (Asn2–Thr248). The *A. aeolicus* TrmI protomer (Fig. 1b) consists of the small N-terminal domain (residues 2–58) and the C-terminal methyltransferase domain (residues 72–248), which are connected by an α-helical linker (residues 59–71). The N-terminal domain forms a small β sandwich (Fig. 1b), in which the β sheet β2–β1–β6–β5 stacks on the β hairpin β3–β4, along with the small 3_{10}-helix η1. The C-terminal domain adopts the typical type I methyltransferase fold, with a central seven-stranded β sheet with the topology β9–β8–β7–β10–β11–β14–β12, flanked by α helices on both sides (Fig. 1b). As reported previously [19], the long β strand β12, in which the head interacts with β13, is characteristic of TrmI among the type I methyltransferases, and it provides a surface for tetramerization.

We analyzed the oligomeric state of *A. aeolicus* TrmI in solution by sedimentation velocity ultracentrifugation. The gel filtration elution profile of *A. aeolicus* TrmI showed one peak between the IgG (158 kDa) and human albumin (66 kDa) markers. Since the theoretical molecular weight of *A. aeolicus* TrmI is 28.7 kDa, TrmI is suggested to exist as tetramer (114.8 kDa) in solution. The ultracentrifugation analysis, using 1 mg/ml *A. aeolicus* TrmI, showed one peak at 110 kDa (Fig. 1c), which confirmed that it is tetrameric in solution.

The methyl donor AdoMet is bound in the C-terminal domain of the protein (Fig. 1b). *A. aeolicus* TrmI recognizes AdoMet by hydrogen bonds from its main-chain and side-chain atoms as well as water-mediated hydrogen bonds (Fig. 1d), in a similar manner to *T. thermophilus* TrmI (Fig. 1e) [19] and *P. abyssi* TrmI (Fig. 1f) [20]. The N1 atom of the adenine moiety hydrogen bonds with the main chain amide nitrogen of Phe149 (3.0 Å) of *A. aeolicus* TrmI. The N6 amino group hydrogen bonds with the side chains of Asp148 (2.9 Å) and Tyr172 (3.1 Å) (Fig. 1d). The N7 atom interacts with a water (wat1 in Fig. 1d; 2.7 Å), which participates in a hydrogen bonding network involving Glu168, Tyr172, and a water (Wat2 in Fig. 1d). In addition to these four hydrogen bonds, the adenine ring forms a T-stacking interaction with the side chain of Phe98, which is fixed by π–π stacking with that of Phe149 (Fig. 1d). The two hydroxyl groups of the ribose moiety of AdoMet interact with the side chain of Glu120 (2.6 and 2.7 Å; Fig. 1d). The methionine moiety of AdoMet forms three hydrogen bonds (Fig. 1d): its amino group hydrogen bonds with the side chain of Asp165 (2.9 Å), and its carboxyl group hydrogen bonds with the main-chain amide nitrogen atoms of Ala104 (3.1 Å) and Leu105 (2.8 Å; Fig. 1d).

We compared the structure of *A. aeolicus* TrmI to those of *T. thermophilus* TrmI in complex with *S*-adenosyl-L-homocysteine (AdoHcy) (Fig. 1e) and *P. abyssi* TrmI in complex with AdoMet (Fig. 1f), and examined the conservation of residues involved in AdoMet binding. *A. aeolicus*, *T. thermophilus*, and *P. abyssi* all live in high-temperature environments. The N6 amino group of the adenine moiety is recognized in diverse manners by the various TrmI structures. The side chains of three amino acid residues (Asp148, Lys150, and Tyr172 in *A. aeolicus* TrmI; Fig. 2) surround the N6 amino group, and the underlined residues are involved in AdoMet binding. In the corresponding three positions, *T. thermophilus* TrmI has Lys153, Glu155, and Val177, while *P. abyssi* TrmI has Asp153, Tyr155, and Val176 (Fig. 2). Asp148 and Tyr172 of *A. aeolicus* TrmI form direct hydrogen bonds with the N6 amino group (Fig. 1d). In *T. thermophilus* TrmI (Fig. 1e) [19], the side chain of Glu155 and a water molecule form hydrogen bonds with the N6 amino group, and these are apparently equivalent to the two hydrogen bonds formed between this moiety and *A. aeolicus* TrmI. However, Glu155 of *T. thermophilus* TrmI is located at a different position than Asp148 of *A. aeolicus* TrmI in the amino acid alignment (Fig. 2). On the other hand, *P. abyssi* TrmI forms only one hydrogen bond by Asp153 (Fig. 1f) [20], which is located at the same position as Asp148 of *A. aeolicus* TrmI (Fig. 2). The distances from the N6 amino group to the three water molecules (Fig. 1f) are 3.8, 3.9, and 5.5 Å, respectively. The N7 atom of AdoMet is bound

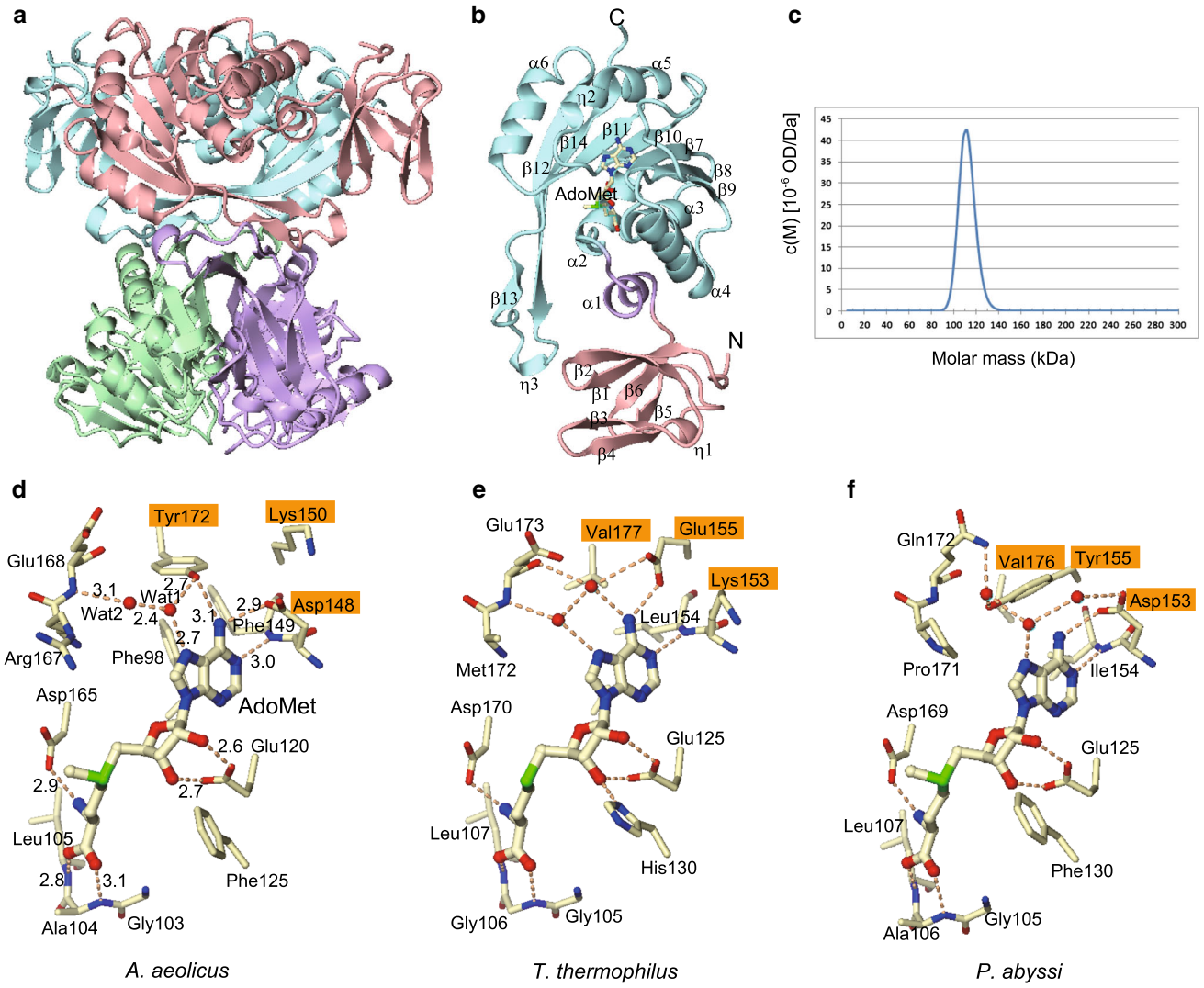

Fig. 1 Crystal structure of *A. aeolicus* TrmI in complex with AdoMet. **a** The tetrameric structure of *A. aeolicus* TrmI. The four protomers are colored *pink*, *cyan*, *purple*, and *green*. **b** Protomer structure of *A. aeolicus* TrmI. The N-terminal domain, the linker helix, and the C-terminal domain are colored *pink*, *purple*, and *cyan*, respectively. The secondary structures are labeled. **c** The calculated distributions c(M) by Sedfit [30]. **d**–**f** *Ball-and-stick* representations of AdoMet binding by *A. aeolicus* TrmI (chain A) (**d**), *T. thermophilus* TrmI [19] (chain A) (**e**), and *P. abyssi* TrmI [20] (chain A) (**f**). The three amino acid residues surrounding the N6 amino group of AdoMet are labeled with *orange rectangles*. Hydrogen bonds are depicted by *dotted lines* with their distances (Å). The figures were created using CueMol (http://cuemol.sourceforge.jp/en/)

to TrmI by one water-mediated hydrogen bond, although the side chains involved in its coordination differ (Fig. 1d–f).

We examined the conservation of these three amino acid residues in the other TrmIs with available structures (Fig. 2). Asp148 of *A. aeolicus* TrmI is conserved in *P. abyssi*, *T. maritima*, *M. tuberculosis*, and *Homo sapiens*. Lys153 in *T. thermophilus* TrmI is an exception. Lys150 of *A. aeolicus* TrmI is not conserved and does not interact with AdoMet. Glu155 of *T. thermophilus* TrmI and Tyr155 of *P. abyssi* TrmI participate in the AdoMet binding in distinct manners. By contrast, Ser175 of *H. sapiens* Trm61 (PDB ID 2B25) is 4.7 Å away from the N6 amino group, and does not interact with AdoMet. The TrmIs from *T. maritima* (PDB ID 1O54) and *M. tuberculosis* (PDB ID 1I9G) have Ser and Ala residues, respectively. Although the only available structure of *T. maritima* TrmI is the substrate-free form, the Ser residue is located too far away to interact with AdoMet. Tyr172 of *A. aeolicus* TrmI is conserved in *M. maritima* TrmI, and is replaced by

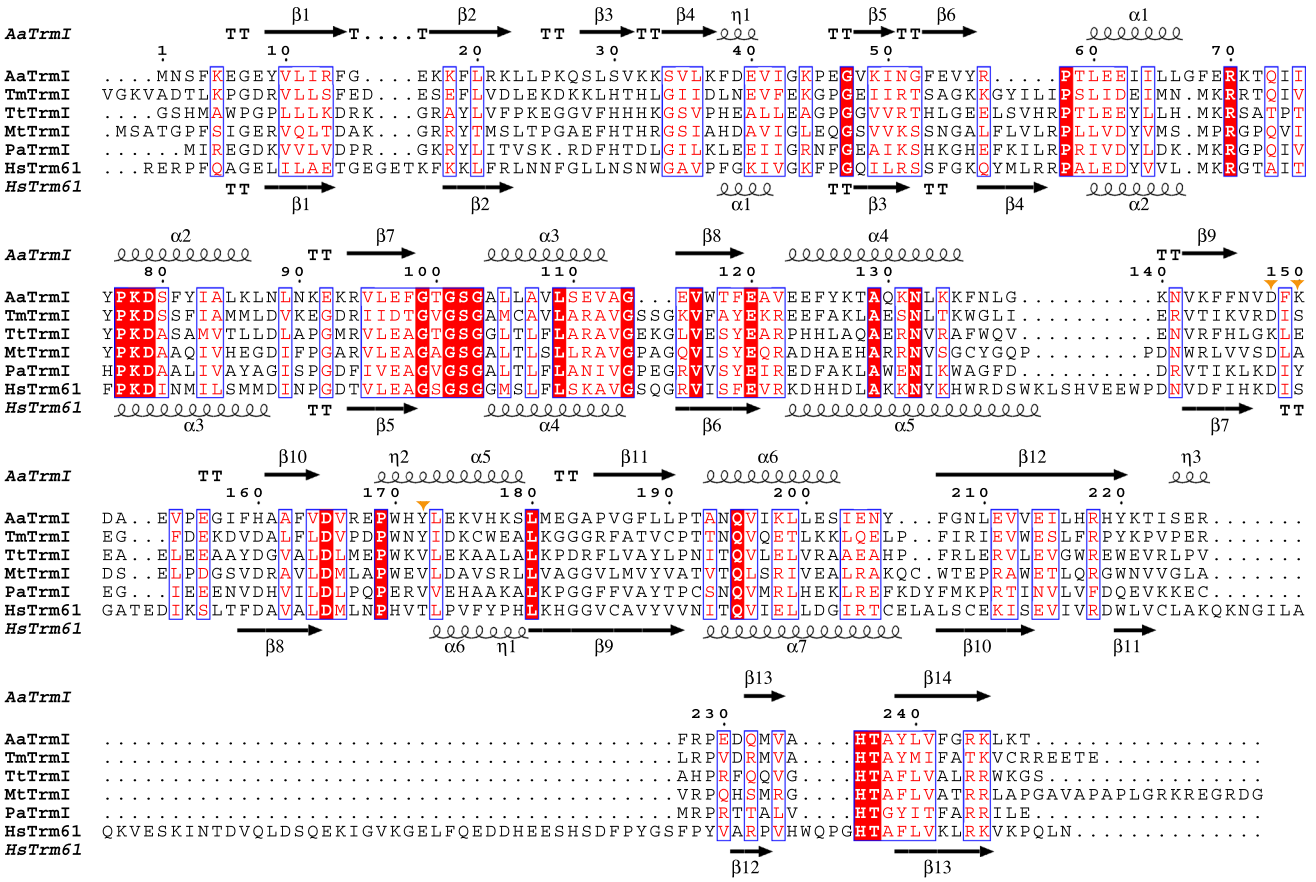

Fig. 2 Sequence alignment of TrmI proteins. The amino acid sequences of *A. aeolicus* TrmI (AaTrmI), *T. maritima* TrmI (TmTrmI), *T. thermophilus* TrmI (TtTrmI), *M. tuberculosis* TrmI (MtTrmI), *P. abyssi* TrmI (PaTrmI), and *H. sapiens* Trm61 (HsTrm61) were aligned with ClustalX 2.1 [31]. Identical residues are *white in a red background*. Similar residues are *red in blue rectangles*. The secondary structures of *A. aeolicus* TrmI (PDB: 2YVL) and *H. sapiens* Trm61 (PDB: 2B25) are shown at the *top* and *bottom*, respectively. The three amino acid residues with side chains located near the N6 amino group of AdoMet are indicated by *orange triangles*. The figure was depicted by ESPript [32]

aliphatic residues in *T. thermophilus* TrmI, *M. tuberculosis* TrmI, and *P. abyssi* TrmI, and by Thr175 in *H. sapiens* Trm61. The side chain of Thr175 is 5.3 Å away from the N6 amino group (PDB ID 2B25), and its hydroxyl group does not coordinate any water molecules.

Two other differences are the presence of T-stacking by Phe98 in *A. aeolicus* TrmI (Fig. 1d), and the additional hydrogen bond to the ribose moiety by His130, observed in *T. thermophilus* TrmI (Fig. 1e). The presence of Phe98 is unique to *A. aeolicus* TrmI (Fig. 2), whereas the His residue at the corresponding position of His130 in *T. thermophilus* TrmI is shared by the *M. tuberculosis* and *H. sapiens* TrmIs. The binding modes for the other part of AdoMet are quite similar. They involve the hydrogen bond between N1 of the adenine moiety to the main-chain amide nitrogen, the interaction between the two hydroxyl groups of the ribose moiety and the Glu side chain, and the binding to the amino and carboxyl groups of the methionine moiety. For the methionine moiety, the Asp165 that interacts with the amino group is conserved, and the conformations of the main-chain amide groups that interact with the carboxyl group are quite similar.

Summary

We have determined the crystal structure of TrmI from the extremely thermophilic bacterium *A. aeolicus*, and examined the similarities and differences regarding the recognition of the methyl donor AdoMet by *A. aeolicus* TrmI and the *T. thermophilus* and *P. abyssi* TrmIs. The recognition of the N6 amino group of the adenine moiety was the most diverse feature. Three residues are located where their side chains can approach the N6 amino group. Our comparative structural analyses revealed the different strategies adopted by these thermophilic species to form hydrogen bonds by using acidic and hydrophilic side chains. It is intriguing that the universal substrate AdoMet has become

recognized in distinct manners by the TrmIs catalyzing the tRNA m^1A58 modification, during the course of evolution.

Acknowledgments The authors thank the staff at beamline BL41XU of SPring-8. We also thank Tomoko Nakayama, Mihoko Iizuka, Shingo Saito, Taichi Mishima, Kaori Yamanaka, Kojiro Ake, Takako Imada, Kazuko Maekawa, Chie Hori-Takemoto, Tomomi Kamo-Uchikubo, Ryogo Akasaka, Chizu Kuroishi, and Takaho Terada for clerical assistance, performing structural genomics/proteomics projects, facility maintenance, and experimental assistance. This research was supported by a grant from the Daiichi-Sankyo Foundation of Life Science (12-039 to Y.B.), Grants-in-Aid for Scientific Research in Priority Areas from the Ministry of Education, Culture, Sports, Science and Technology (MEXT) of Japan (to S.Y.), and by the RIKEN Structural Genomics/Proteomics Initiative (RSGI) in the National Project on Protein Structural and Functional Analyses, MEXT of Japan (to S.Y.).

References

1. Sprinzl M, Vassilenko KS (2005) Compilation of tRNA sequences and sequences of tRNA genes. Nucleic Acids Res 33(Database issue):D39–D40
2. Gilboa E, Goff S, Shields A, Yoshimura F, Mitra S, Baltimore D (1979) In vitro synthesis of a 9 kbp terminally redundant DNA carrying the infectivity of Moloney murine leukemia virus. Cell 16(4):863–874
3. Maden BE (1990) The numerous modified nucleotides in eukaryotic ribosomal RNA. Prog Nucleic Acid Res Mol Biol 39:241–303
4. Burnett BP, McHenry CS (1997) Posttranscriptional modification of retroviral primers is required for late stages of DNA replication. Proc Natl Acad Sci USA 94(14):7210–7215
5. Renda MJ, Rosenblatt JD, Klimatcheva E, Demeter LM, Bambara RA, Planelles V (2001) Mutation of the methylated $tRNA_3^{Lys}$ residue A58 disrupts reverse transcription and inhibits replication of human immunodeficiency virus type 1. J Virol 75(20):9671–9678
6. Helm M, Giege R, Florentz C (1999) A Watson-Crick base-pair-disrupting methyl group (m^1A9) is sufficient for cloverleaf folding of human mitochondrial $tRNA^{Lys}$. Biochemistry 38(40):13338–13346
7. Hayrapetyan A, Seidu-Larry S, Helm M (2009) Function of Modified Nucleosides in RNA stabilization. In: Grosjean H (ed) DNA and RNA modification enzymes: comparative structure, mechanism, functions, cellular interactions and evolution, chapter 37. LANDES Biosci, USA
8. Anderson J, Phan L, Cuesta R, Carlson BA, Pak M, Asano K, Bjork GR, Tamame M, Hinnebusch AG (1998) The essential Gcd10p-Gcd14p nuclear complex is required for 1-methyladenosine modification and maturation of initiator methionyl-tRNA. Genes Dev 12(23):3650–3662
9. Kim SH, Suddath FL, Quigley GJ, McPherson A, Sussman JL, Wang AH, Seeman NC, Rich A (1974) Three-dimensional tertiary structure of yeast phenylalanine transfer RNA. Science 185(4149):435–440
10. Robertus JD, Ladner JE, Finch JT, Rhodes D, Brown RS, Clark BF, Klug A (1974) Structure of yeast phenylalanine tRNA at 3 Å resolution. Nature 250(467):546–551
11. Schevitz RW, Podjarny AD, Krishnamachari N, Hughes JJ, Sigler PB, Sussman JL (1979) Crystal structure of a eukaryotic initiator tRNA. Nature 278(5700):188–190
12. Droogmans L, Roovers M, Bujnicki JM, Tricot C, Hartsch T, Stalon V, Grosjean H (2003) Cloning and characterization of tRNA (m^1A58) methyltransferase (TrmI) from *Thermus thermophilus* HB27, a protein required for cell growth at extreme temperatures. Nucleic Acids Res 31(8):2148–2156
13. Sierzputowska-Gracz H, Gopal HD, Agris PF (1986) Comparative structural analysis of 1-methyladenosine, 7-methylguanosine, ethenoadenosine and their protonated salts IV: ^1H, ^{13}C, and ^{15}N NMR studies at natural isotope abundance. Nucleic Acids Res 14(19):7783–7801
14. Agris PF, Sierzputowska-Gracz H, Smith C (1986) Transfer RNA contains sites of localized positive charge: carbon NMR studies of [^{13}C]methyl-enriched *Escherichia coli* and yeast $tRNA^{Phe}$. Biochemistry 25(18):5126–5131
15. Anderson J, Droogmans L (2005) Biosynthesis and function of 1-methyladenosine in transfer RNA. In: Grosjean H (ed) Fine-tuning of RNA functions by modification and editing. Springer, Berlin, pp 121–139
16. Gupta A, Kumar PH, Dineshkumar TK, Varshney U, Subramanya HS (2001) Crystal structure of Rv2118c: an AdoMet-dependent methyltransferase from *Mycobacterium tuberculosis* H37Rv. J Mol Biol 312(2):381–391
17. Bujnicki JM (2001) In silico analysis of the tRNA:m1A58 methyltransferase family: homology-based fold prediction and identification of new members from Eubacteria and Archaea. FEBS Lett 507(2):123–127
18. Roovers M, Wouters J, Bujnicki JM, Tricot C, Stalon V, Grosjean H, Droogmans L (2004) A primordial RNA modification enzyme: the case of tRNA (m^1A) methyltransferase. Nucleic Acids Res 32(2):465–476
19. Barraud P, Golinelli-Pimpaneau B, Atmanene C, Sanglier S, Van Dorsselaer A, Droogmans L, Dardel F, Tisne C (2008) Crystal structure of *Thermus thermophilus* tRNA m^1A_{58} methyltransferase and biophysical characterization of its interaction with tRNA. J Mol Biol 377(2):535–550
20. Guelorget A, Roovers M, Guerineau V, Barbey C, Li X, Golinelli-Pimpaneau B (2010) Insights into the hyperthermostability and unusual region-specificity of archaeal *Pyrococcus abyssi* tRNA $m^1A57/58$ methyltransferase. Nucleic Acids Res 38(18):6206–6218
21. Guelorget A, Barraud P, Tisne C, Golinelli-Pimpaneau B (2011) Structural comparison of tRNA m^1A58 methyltransferases revealed different molecular strategies to maintain their oligomeric architecture under extreme conditions. BMC Struct Biol 11:48
22. Baker EN (2007) Structural genomics as an approach towards understanding the biology of tuberculosis. J Struct Funct Genomics 8(2–3):57–65
23. Sugahara M, Asada Y, Shimizu K, Yamamoto H, Lokanath NK, Mizutani H, Bagautdinov B, Matsuura Y, Taketa M, Kageyama Y, Ono N, Morikawa Y, Tanaka Y, Shimada H, Nakamoto T, Sugahara M, Yamamoto M, Kunishima N (2008) High-throughput crystallization-to-structure pipeline at RIKEN SPring-8 Center. J Struct Funct Genomics 9(1–4):21–28
24. Yokoyama S, Kigawa T, Shirouzu M, Miyano M, Kuramitsu S (2008) RIKEN structural genomics/proteomics initiative. Tanpakushitsu Kakusan Koso 53(5):632–637
25. Terwilliger TC (2011) The success of structural genomics. J Struct Funct Genomics 12(2):43–44

26. Otwinowski Z, Minor W (1997) Processing of X-ray diffraction data collected in oscillation mode. Academic Press, New York
27. Collaborative Computational Project Number 4 (1994) The CCP4 suite: programs for protein crystallography. Acta Crystallogr D50:760–763
28. Emsley P, Cowtan K (2004) Coot: model-building tools for molecular graphics. Acta Crystallogr D60:2126–2132
29. Murshudov GN, Vagin AA, Dodson EJ (1997) Refinement of macromolecular structures by the maximum-likelihood method. Acta Crystallogr D53:240–255
30. Schuck P (2000) Size-distribution analysis of macromolecules by sedimentation velocity ultracentrifugation and lamm equation modeling. Biophys J 78(3):1606–1619
31. Larkin MA, Blackshields G, Brown NP, Chenna R, McGettigan PA, McWilliam H, Valentin F, Wallace IM, Wilm A, Lopez R, Thompson JD, Gibson TJ, Higgins DG (2007) Clustal W and Clustal X version 2.0. Bioinformatics (Oxford, England) 23(21):2947–2948
32. Gouet P, Courcelle E, Stuart DI, Metoz F (1999) ESPript: analysis of multiple sequence alignments in PostScript. Bioinformatics (Oxford, England) 15(4):305–308